Fragment Mass Distribution of Platelike Objects

Toshihiko Kadono
Institute of Space and Astronautical Science, Kanagawa 229, Japan
and Department of Physics, Kyoto University, Kyoto 606, Japan
(Received 30 November 1995; revised manuscript received 30 August 1996)

The fragment mass distributions of platelike objects are investigated by conducting two types of experiments. The first is a "sandwich" experiment in which thin glass and plaster plates are inserted between two larger stainless steel plates and an iron projectile is dropped onto the target plate at normal incidence. The second is a "lateral impact" experiment in which a hypervelocity nylon projectile collides at the side of the plaster plates. There is a discrepancy in the power-law exponent of fragment mass distribution between the sandwich experiment and the lateral impact experiment. A model that agrees with the experimental results is proposed. [S0031-9007(97)02420-4]

PACS numbers: 46.30.Nz

Dynamic fragmentation of solid bodies caused by hypervelocity impact or explosion has been investigated over many decades in various fields including engineering and planetary sciences [1,2]. The experiments of the dynamic fragmentation have been conducted mainly using a three-dimensional (3D) target such as a sphere or cube. For such 3D targets, three-dimensional components of the stress induce various and intricate fragmentation processes. This situation is too complex to investigate the fragmentation phenomenon in detail. Recently, fragmentation experiments of platelike objects were carried out to derive the fragment mass distributions [3–6]. Oddershede, Dimon, and Bohr [4] and Meibom and Balslev [6] reported that the fragmentation of a platelike object by letting it fall onto a hard floor indicated a power law with the exponent α about 0.2 in the cumulative distribution $N(>m)$ defined as the number of fragments with mass larger than m. On the other hand, Neda, Mocsy, and Bako [5] observed by letting the plates fall onto a concrete floor that α changed with the energy input and became about 0.8.

In these experiments, the fragmentation was mainly induced by bending the objects in the 3D space. However, in the 2D space the fragmentation caused by the bending of the objects out of the plate plane does not occur and the forces producing the fragments are restricted on the plate plane. Here two types of the fragmentation experiments are conducted. First, we carried out the "sandwich" experiments by using thin glass (100 mm diameter and 1 mm thickness) and plaster (100 mm diameter and 2.5 mm thickness) plates which were placed between two larger sized plates of stainless steel. Spherical iron projectile of diameter 100 mm was dropped from various heights and collided with a stainless cylinder with the diameter of 100 mm vertically; the cylinder was placed on the stainless steel plate in order to load a force uniformly. Grady and Kipp [3] also performed the sandwich experiment but they paid most attention to the distribution of larger fragments rather than the power-law distribution of the small fragments.

Second, we carried out the "lateral impact" experiments by colliding a hypervelocity projectile ($\sim$4 km/s) to the side of plates. The stress wave propagating from the impact point generates a new crack surface perpendicular to the plate plane rather than a parallel crack surface when the plate is thin enough. Within the distance about target thickness from the impact point "3D fragments" which have only one or no surface of the original target plate were produced. However, outside of this area, no 3D fragment exists and "2D fragments" which have both top and bottom surfaces of the original plate were generated [all fragments shown in Fig. 1(b) are the 2D fragments]. Also, the crack propagation velocity in hypervelocity impact fragmentation is about the sound velocity of the target material, which is $\sim$1 km/s, so that the target does not have a time to bend and the fragmentation due to the bending cannot occur. It should be noted that in the 2D space all forces should be loaded through a boundary (side) of the plate in the plane where the object exists such as the lateral impact, and that the fragmentation caused by the force which works normally to the plate plane is not realized.

The lateral impact experiments were done using spherical nylon projectiles with the diameter of 7 mm and the mass of 0.21 g; they were accelerated by a two-stage light-gas gun at the Institute of Space and Astronautical Science (ISAS). We used plaster as target material in order to mold various shapes and prepared the target plates with the diameters ranging from 95 to 308 mm and the thicknesses from 3.3 to 14 mm. The targets were horizontally installed between acrylic resin plates of 5 mm thickness. Between the acrylic resin plates washers that had the same thickness as the target were inserted. The target was not fixed and could move horizontally between the acrylic resin plates. It was set inside a plastic box that had an entrance hole of 15 mm diameter and was lined with urethane foam in order to prevent secondary disruptions of the fragments. The projectile passed through the entrance hole and impacted on the side of the target. The first series of the lateral impact experiment was carried out with targets of

 0031-9007/97/78(8)/1444(4)$10.00

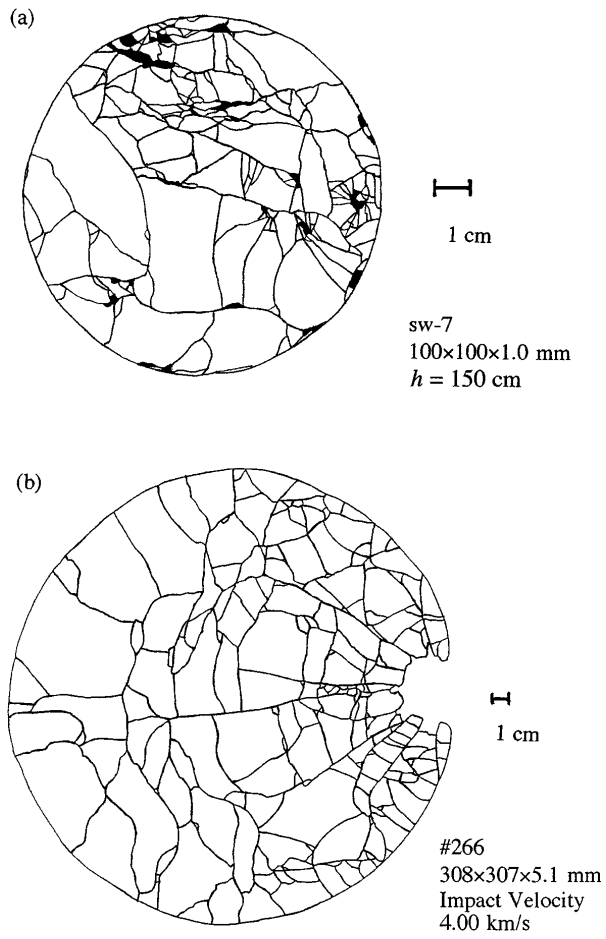

FIG. 1. Sketch of crack patterns. (a) Pattern produced by a sandwich experiment for glass plate. The iron projectile is dropped from the height 150 cm. The areas where we cannot find suitable fragments are indicated as shadows. (b) Pattern produced by impacting the hypervelocity projectile at the side of the plaster plate. Projectile was shot from the right. All fragments shown in this figure are the 2D fragments. Two kinds of large cracks, radial cracks and cracks perpendicular to the radial ones, are produced. The experimental conditions are shown in the figure.

various diameters and thicknesses at a constant velocity of 4 ± 0.4 km/s. The second series was conducted by changing the velocity of the projectiles (0.6–4.1 km/s) and used the targets with the 200 mm diameter and the 5 mm thickness. We also did the hypervelocity impact experiments with the spherical targets for comparison. All these experiments were performed under an ambient pressure of about 1 Torr.

After the experiments, fragments were collected and reconstructed to investigate the pattern of the large cracks. Figure 1 shows sketches of crack patterns. The crack pattern of a glass target in Fig. 1(a) seems to have occurred at random. On the other hand, the crack pattern caused by the lateral impact is shown in Fig. 1(b), and two kinds of cracks are recognized: radial cracks initiating from the impact point and cracks perpendicular to the radial ones. Because most of the perpendicular cracks do not traverse the radial cracks, the radial cracks are considered to be formed prior to the perpendicular ones.

The mass of the 2D fragments that were weighed more than 2–3 mg was measured. Most fragments of the glass plate heavier than 2–3 mg are 2D fragments while most 2D fragments of the plaster plate are weighed more than 10 mg. Figure 2(a) shows $N(>m)$ resulting from the glass plate sandwich experiments with various heights h from which the projectile is dropped, 15, 75, and 120 cm, against the fragment masses normalized by the original target mass. It can be seen that the slope for the smaller fragments ($m < 0.01$) for $h = 15$ cm is different from the others. Figure 2(b) shows $N(>m)$ resulting from the plaster plate sandwich experiments with $h = 30$ and 150 cm. Two distributions for $h = 150$ cm are shown; the open circle is for the 2D fragment distribution, and the filled circle is for the distribution of all the fragments larger than the minimum 2D fragment mass. It is seen that the slope for the smaller fragment for $h = 30$ cm is different from that for 150 cm. On the other hand, $N(>m)$ shown in Fig. 2(c) was produced by the lateral impact. The open circle is for the 2D fragment distribution, and the filled circle is for the distribution of all the fragments larger than the minimum 2D fragment mass.

We fit $N(>m)$ as

$$N(>m) = A \exp(-m/m_0) m^{-\alpha}, \qquad (1)$$

where A, m_0, and α are constants. The exponent α characterizes a power-law behavior for smaller fragments. Figure 3(a) shows α found by the sandwich experiments against the largest fragment masses. It can be thought that the largest fragment mass is related to the degree

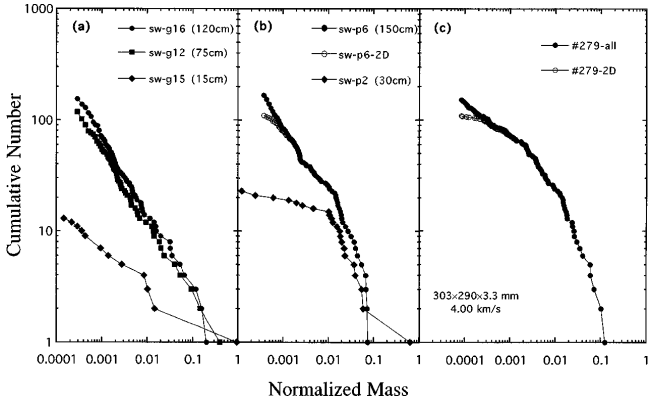

FIG. 2. (a) $N(>m)$ resulting from the glass plate sandwich experiments against the fragment masses normalized by the original target mass for $h = 15$, 75, and 120 cm. (b) $N(>m)$ resulting from the plaster plate sandwich experiments for $h = 30$ and 150 cm. Two distributions for 150 cm are shown; the open circle is for the 2D fragment distribution and the filled circle is for the distribution of all the fragments larger than the minimum 2D fragment mass. (c) $N(>m)$ resulting from the lateral impact. The open circle is for the 2D fragment distribution, and the filled circle is for the distribution of all the fragments larger than the minimum 2D fragment mass.

of fragmentation. This figure indicates that α increases as the degree of fragmentation increases (or the largest mass decreases). For the large degree of fragmentation, α exceeds 0.5 and becomes 0.5–0.7.

In Fig. 3(b) the exponents α in the lateral impact experiments are plotted against the largest fragment masses, including the two cases of spherical targets. The upper limit of α is obtained from the distribution of all the fragments larger than the minimum 2D fragment mass, while the lower limit is from the 2D fragments. The results of three types of the target diameter are shown: below 15 cm (filled circle), 15–25 cm (filled square), and larger than 25 cm (filled triangle). For noncircular targets, the average size of the major axis and the minor axis is defined as the diameter. The measured exponents are about 0.1–0.3 regardless of the largest fragment mass and the target size. Figure 3(b) also includes α in the second series of the lateral impact experiments of the 200 mm diameter and the 5 mm thickness plate with various impact velocities 0.60, 1.33, 2.70, 3.85, and 4.10 km/s as indicated by open squares. It seems that the exponent α is almost constant even if the input kinetic energy increases by a factor of about 50. Figure 4 shows the exponents in the lateral impact experiments against the ratio of the target diameter to the thickness. As the ratio increases, the effects of 3D fragments (the difference between the upper and the lower limits) seem to decrease.

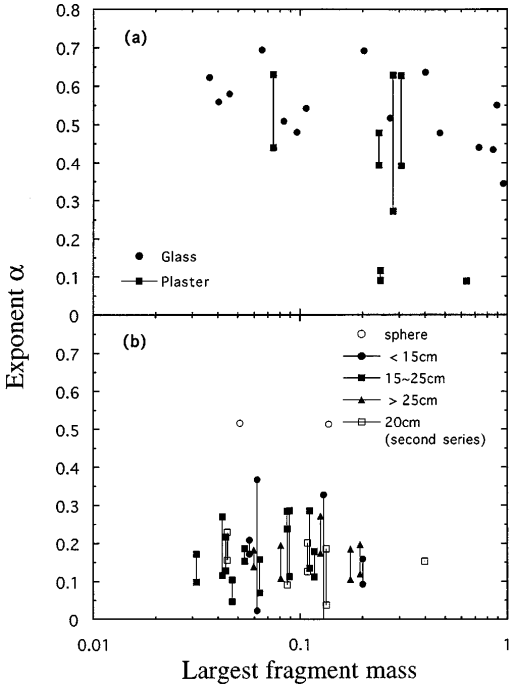

FIG. 3. (a) The exponents α in the glass and plaster plate sandwich experiments against the largest fragment masses. With decreasing the largest mass, α increases. For the small largest mass, α exceeds 0.5. (b) The exponents α in the lateral impact experiments, including two cases of spherical targets (open circles). Their upper limit is obtained from the distribution of all the fragments larger than the minimum 2D fragment while the lower limit is from the 2D fragments. The results of three types of the target diameter are shown: below 15 cm (filled circle), 15–25 cm (filled square), and larger than 25 cm (filled triangle). The exponents in the second series of the lateral impact experiments using the 200 mm diameter and 5 mm thickness plaster plate with various impact velocities 0.60, 1.33, 2.70, 3.85, and 4.10 km/s are indicated by open squares. The measured exponents are about 0.1–0.3 regardless of the largest fragment mass, the target size, and the energy input.

Thus, in the sandwich experiments α varies with the energy input and approaches to about 0.5–0.7, while that in the lateral impact experiments is about 0.1–0.3 regardless of the energy input. It should be noted that it is difficult to determine α exactly because of its large scatter as ambiguity always exists in the fragmentation experiment like that α in the spherical target fragmentation is not always exactly the same value.

Various theoretical fragment mass distributions have been proposed [3,7–14], but a theory to satisfy these experimental results is not yet available. Let us estimate the exponent α by a simple model. The differential fragment mass distribution is assumed to be $n(m)dm = Am^{-\alpha-1}dm$, where A is a constant and the mass m is normalized by the original target mass M_t, and we define an energy density $\varepsilon \equiv E/M_t$, where E is the total input energy.

First we estimate α in the lateral impact case. The stress wave propagates from the impact point. After the passing of the stress wave, the stress magnitude increases, and then the cracks grow, new cracks are generated, and the fragments are produced; as a result, the stress is released. Consider that a fragment with the length $l \propto m^{1/d}$, where d is the dimension of space, is separated from an adjacent fragment with a relative velocity v_{rel}. The principal source of energy available to drive the fractures is the kinetic energy of the material arising from motion relative to the center of mass. The kinetic

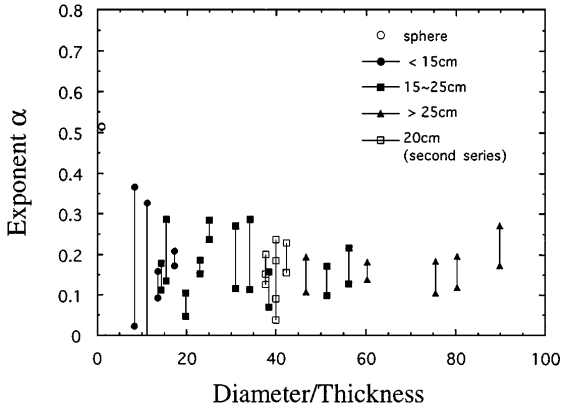

FIG. 4. The exponents in the lateral impact experiments against the ratio of the target diameter to the thickness. As the ratio increases, the effects of 3D fragments (the difference between the upper and the lower limits) decrease.

energy about the center of mass can be written as $m v_{\rm rel}{}^2$. A fracture energy of $\sigma m^{1-1/d}$, where σ is the surface energy density, is consumed at the new surface of the fragment from the energy supply within the fragment. If this is assumed to be equal to the kinetic energy then $v_{\rm rel}{}^2 \propto m^{-1/d}$. The fragment separates when the strain $\Delta l/l$ exceeds a critical value. The strain $\Delta l/l$ is equal to $(\Delta l/\Delta t)(\Delta t/l) \cong v_{\rm rel}(\Delta t/l)$, where Δt is a time required for the fragment to expand Δl from the rest. Thus Δt is estimated approximately as $\Delta t \propto m^{1/d}/v_{\rm rel} \propto m^{3/2d}$. Consider a small sized region in the target. The stress in this region is released during approximately $\Delta t_L \propto m_L{}^{3/2d}$, where m_L is the mass of the largest fragment generated in this region. Hence the mass released from the high stress per unit time becomes,

$$\dot{m} \propto \frac{1}{\Delta t_L} \int_0^{m_L} mAm^{-\alpha-1} dm \propto m_L^{1-3/2d-\alpha}. \quad (2)$$

If the crack growth process is steady state, the crack-filled region grows in the direction of the stress wave propagation with a constant velocity; that is, the mass (volume) invaded by the cracks per unit time is constant. Therefore the right-hand side of Eq. (2) should be independent of m_L so that the exponent $1 - 3/2d - \alpha$ should be equal to 0: $\alpha = 1 - 3/2d$. In the case of $d = 2$, α becomes 0.25. This is consistent with the results of the lateral impact experiments. Hayakawa [14] constructed a model in a similar manner, in which the total fragment mass within "thickness" L was proportional to L so that a larger exponent ($\alpha = 0.5$) for planar wave propagation was derived.

On the other hand, in the sandwich experiment the force is applied to the plate plane uniformly and simultaneously. The stress is loaded during a constant time Δt_s at any locations of the target. Hence the mass released per unit time is estimated as

$$\dot{m} = \frac{1}{\Delta t_s} = \frac{1}{\Delta t_s} \int_0^{m_L} mAm^{-\alpha-1}\, dm \propto \int_0^{m_L} m^{-\alpha} dm\,. \quad (3)$$

The integration in Eq. (3) is equal to the original target mass and should be finite so that the exponent α is necessary to satisfy $1 > \alpha$, otherwise the integration may diverge. Also, the input energy is mainly spent in production of new crack surfaces in the sandwich experiment. Consider a case of large ε. Since surface energy of a fragment can be written as $\sigma m^{-(d-1)/d}$, we can write

$$\varepsilon \propto \int_0^{m_t} \sigma m^{(d-1)/d} Am^{-\alpha-1}\, dm \propto \int_0^{m_L} m^{-1/d-\alpha} dm\,. \quad (4)$$

If $1 > \alpha + 1/d$, the right-hand side of Eq. (4) has an upper limit though ε can be an arbitrary large value. Hence, $1 \le \alpha + 1/d$ should be satisfied and then $1 - 1/d \le \alpha$. In the case of $d = 2$, it becomes $0.5 \le \alpha$. Thus we obtain $0.5 \le \alpha \le 1$ in the case of the sandwich experiment. This is consistent with the results of the sandwich experiments. It should be noted that in the lateral impact the input energy is transformed into not only the new surface formation but also the kinetic energy of the fragments. At present we do not know the dependence of the kinetic energy on the fragment mass so that we cannot obtain a constraint from the energy conservation.

Finally the experiment in which a projectile impacts at the side of the plates at higher velocity (>5 km/s) should be done to confirm that α does not vary at the higher degree of fragmentation. Unfortunately, the two-stage light-gas gun at ISAS cannot accelerate the projectile faster than 5 km/s so that α cannot be observed at larger input energy.

In summary, the power-law exponent α in the sandwich experiments using thin glass and plaster plates increased with the energy input and became 0.5–0.7, while that in the fragmentation by impacting a hypervelocity projectile at the side of the plaster plate was 0.1–0.3 regardless of the energy input. We derive $\alpha = 0.25$ in the lateral impact fragmentation from a simple model. Also we estimate the possible range of the exponent in the sandwich experiment, 0.5–1.0. These are consistent with the experimental results.

The author thanks A. M. Nakamura, A. Fujiwara, H. Yano, S. Shirono, T. Yamamoto, H. Suto, T. Sugiyama, H. Sogawa, and H. Mizutani for helpful comments and discussions.

[1] D. R. Curran, L. Seaman, and D. A. Shockey, Phys. Rep. **147**, 253 (1987).
[2] A. Fujiwara, P. Cerroni, D. Davis, E. Ryan, M. Di Martino, K. Holsapple, and K. Housen, in *Asteroid II*, edited by R. P. Binzel, T. Gehrels, and M. S. Matthews (University of Arizona Press, Tucson, 1989), p. 240.
[3] D. E. Grady and M. E. Kipp, J. Appl. Phys. **58**, 1210 (1985).
[4] L. Oddershede, P. Dimon, and J. Bohr, Phys. Rev. Lett. **71**, 3107 (1993).
[5] Z. Neda, A. Mocsy, and B. Bako, Mater. Sci. Eng. A **169**, L1 (1993).
[6] A. Meibom and I. Balslev, Phys. Rev. Lett. **76**, 2492 (1996).
[7] D. L. Turcotte, J. Geophys. Res. **91**, 1921 (1986).
[8] N. F. Mott, Proc. R. Soc. London **189**, 300 (1947).
[9] J. J. Gilvarry, J. Appl. Phys. **32**, 391 (1961).
[10] T. Kiang, Z. Astrophys. **64**, 433 (1966).
[11] R. Englman, N. Rivier, and Z. Jaeger, J. Appl. Phys. **63**, 4766 (1988).
[12] D. E. Grady, J. Appl. Phys. **68**, 6099 (1990).
[13] L. Baker, A. J. Giancola, and F. Allahdadi, J. Appl. Phys. **72**, 2724 (1992).
[14] Y. Hayakawa, Phys. Rev. B **53**, 14 828 (1996).